Optimization of Glides for Constant Wind Fields and Course Headings

Scott A. Jenkins* and Joseph Wasyl†
University of California at San Diego, La Jolla, California 92093

Theory and experiment are presented for optimal combinations of glide speeds and crab angles that minimize the glide slope at any arbitrary angle to the wind along a constant course heading. The optimization scheme is formulated for constant wind speeds, wind direction, and air mass sink rates. An analytic solution is found in the asymptotic limit of a small crosswind component. A general solution is obtained by seeded iterations with a Taylor series expansion about that limit. The solution was verified in test flights with quartering tailwinds and direct crosswinds at the 700, 500, and 300 mb levels. It was concluded that relatively small pilot-induced speed errors result in significant glide slope degradations with unnecessary and potentially dangerous altitude losses. Applications of the results are considered for wind fields that vary slowly in space, such as lee waves and Rossby waves.

Nomenclature

A_0 = wing area, ft^2
A, B, A′, B′, G = flight path way points
a, b, c = glide polar coefficients at altitude
$\hat{a}, \hat{b}, \hat{c}$ = glide polar coefficients at sea level
C_D = quadratic drag coefficient
$C_{D,i}$ = quadratic induced drag coefficient
$C_{D,p}$ = quadratic profile drag coefficient
C_L = quadratic lift coefficient
d_n, f_n = resolvent cubic parameters for iterative general solution
d_0, f_0 = resolvent cubic parameters for weak crosswinds
K_1 = profile drag factor
K_2 = induced drag factor
K_3 = glide polar factor due to profile drag
K_4 = glide polar factor due to induced drag
L/D = inverse glide slope
$L/D_{\max}$ = inverse glide slope due to speed to fly
$L/D\ (u = U + \delta U)$ = inverse glide slope due to speed-to-fly errors
l = wing cord, n.mi.
m = gross weight, lb
n = integral index number
p_n = second-order coefficient for general iterative case
p_0 = second-order coefficient for weak crosswinds
q_n = first-order coefficient for general iterative case
q_0 = first-order coefficient for weak crosswinds
R = Rossby radius of deformation, n.mi.
r_n = zero-order coefficient for general iterative case
r_0 = zero-order coefficient for weak crosswinds
S = air mass sink rate, kt
U = speed-to-fly at altitude, kt
$\hat{U}$ = speed-to-fly at sea level in still air, kt
U_i = indicated speed-to-fly, kt
U_n = general speed-to-fly for nth wind increment, kt
U_0 = speed to fly in weak crosswinds, kt
u = horizontal component of glide velocity relative to air at altitude, kt
$\hat{u}$ = horizontal component of glide velocity relative to air at sea level, kt
u_s = stall speed, kt
v = wind speed, kt
v_0 = weak wind speed, kt
w = vertical component of glide velocity relative to air at altitude, relative sinking speed in knots
$\hat{w}$ = vertical component of glide velocity relative to air at sea level, relative sinking speed in knots
x = position along flight path relative to any given way point
α = wind angle relative to course line
β = crab angle relative to course line
γ = profile drag exponent
δU = speed-to-fly error, kt
δv = wind speed increment, kt
η = relative squared crosswind velocity difference, kt^2
θ = minimum glide slope in still air at sea level
λ = wave length, n.mi.
ρ = density at altitude, slug/ft^3
$\hat{\rho}$ = density at sea level, slug/ ft^3

Introduction

THE first treatment of the problem of the optimal glide speed that minimizes the glide slope in a moving atmosphere was due to MacCready.[1,2] The solutions have since been referred to as "speed-to-fly." MacCready's original work was valid only for a convective atmosphere in which regions of rising or sinking air translate horizontally with the wind. His speed-to-fly solutions were thus independent of the wind speed and determined uniquely by the rate of vertical air mass movement and the glide polar in still air at sea level.

Subsequently, Kuettner,[3] following arguments introduced by Reichmann,[4] considered the effects on glide slope minimization when regions of rising or sinking air do not translate with the wind over the ground. Such a condition is typically encountered in both hydrostatic and nonhydrostatic lee waves (see Ref. 5). Kuettner considered only the cases of glides directly with the wind. The solutions for speed-to-fly by both Kuettner and Reichmann were graphical in nature, involving tangent plotting for a few selected cases with no mathematics as such presented. Even so, some striking departures from MacCready's original findings were uncovered by both authors. Speed-to-fly was found to be dependent on the wind

Received Dec. 4, 1989; revision received Feb. 13, 1989.

*Research Engineer and Lecturer, Department of Scripps Institution of Oceanography.
†Development Engineer, Department of Scripps Institution of Oceanography.

speed with the flattest glide slopes achieved for tailwinds at speeds less than the MacCready speed-to-fly. Kuettner also considered the degradation in glide slope at high altitudes with a direct tailwind. He concluded that the practice of ballasting to high wing loadings is disadvantageous since the reduced air density at high altitudes has already effectively raised the wing loading considerably. The increase in relative sinking speeds at these higher wing loadings cannot be compensated in downwind glides because slow speeds-to-fly are required.

In the present paper, the speed-to-fly problem is treated for the general case of glides along constant course headings at an arbitrary angle to the wind for any given altitude. Optimal flight paths for crossing lee waves are shown to result from an orthogonal series of constant course glides. The formulation of the problem is based on a quadratic glide polar in a constant wind field. The constant wind-field assumption provides acceptable accuracy for treating glides in lee waves and Rossby waves, which vary over geophysical length scales. The resulting speed-to-fly equation is, nonetheless, found to be transcendental. An asymptotic analytic solution is found in the limit of small crosswind components. A general solution for arbitrary crosswind components is then developed based on a seeded iteration with a Taylor series expansion about the weak crosswind solution. The results are compared with data from skewed test glides performed between the 700- and 300-mb levels. These comparisons show that speed-to-fly errors can degrade the glide slope to such an extent that the performance gains achieved by modern airfoils and composite construction are lost.

Formulation

Consider glides performed at 1-g load factor across a field of lee waves in such a manner that a constant course heading is maintained between any two arbitrary points (A,B) in an Eulerian frame. Let the course heading connecting (A,B) be at an angle α to the wind whose speed is v as shown in Fig. 1. If the horizontal component of the glide velocity relative to the air is u, then it must be directed at some crab angle β in order to maintain a constant course heading between (A,B). The crab angle is thus given by:

$$\beta = \sin^{-1}[-(v/u)\sin\alpha] \tag{1}$$

While traversing the lee wave field, regions of rising flow (lift) will be encountered along the upwind faces of the lee wave crests, and descending flow (sink) along the downwind faces. Let the vertical velocity component of the air mass be S, which shall be taken as positive in the downward direction in an Eulerian frame. If the vertical component of the glide velocity relative to the air is w (positive downward), then the inverse glide slope (L/D) with respect to an Eulerian frame such as the ground will be

$$L/D = \frac{v\cos\alpha + u\cos\beta}{w+S} = \frac{v\cos\alpha + \sqrt{u^2 - v^2\sin^2\alpha}}{w+S} \tag{2}$$

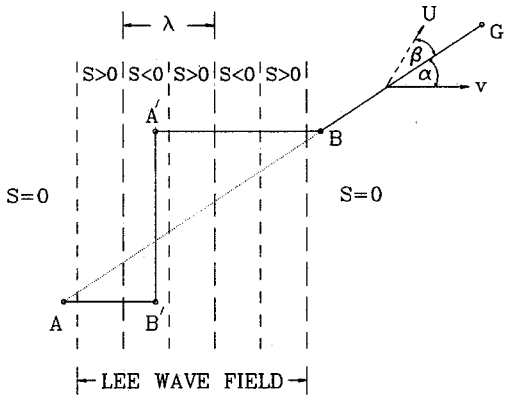

Fig. 1 Schematic of constant course strategies with lee waves.

Any optimal strategy for crossing a field of lee waves is given by one or more glides along constant course headings. This is because the lee wave field structures the air mass sink rates in parallel bands having high cross-stream coherence. Within the lee wave field, an orthogonal series of constant course glides yields the optimum flight path between any two points (A,B) that are separated by some streamwise excursion (see Fig. 1). It is clear from inspection of Eq. (2) that straight line glides with a direct tailwind, $\alpha = 0$, give the maximum possible L/D when entering the lee waves along (A,B′) or when traversing the lee wave field along (A′,B). These two glides can be joined by a direct crosswind glide at constant course heading, (B′,A′), utilizing lee wave lift to achieve an infinite L/D when $S \to -w$. However, sufficiently long crosswind glides in uninterrupted lift such as (B′,A′) are not always possible. Variations in the alignment and width of wave generating mountains often destroy the necessary cross-stream coherence of the lee wave field. If the ultimate goal is significantly far downwind, say point G in Fig. 1, then skewed, constant course glides such as (B, G) will become an inevitable part of cross-country strategy.

Before proceeding to optimize any of the constant course glides set forth in Fig. 1, it is desirable to eliminate w from Eq. (2) in order to save labor. The vertical and horizontal components of the glide velocity relative to the air mass are related by the glide polar at sea level in still air. This relation can be posed from the usual assumption that the total drag is a linear combination of profile drag and induced drag:

$$C_D = C_{D,p} + C_{D,i} \tag{3}$$

Because of Reynolds number dependence, the profile drag coefficient is not constant but will vary with the glide velocity in still air at sea level $\hat{u}$ according to

$$C_{D,p} = K_1\hat{u}^{-\gamma} \tag{4}$$

where K_1 is a factor that varies with the kinematic viscosity and characteristic length scale and γ will depend on the relative proportion of the total wetted surface area that is subjected to laminar vs turbulent boundary layers. The induced drag coefficient on the other hand may be inferred from lifting line theory[6,7] as

$$C_{D,i} = K_2C_L^2 \tag{5}$$

where the factor K_2 is a function of wing aspect ratio, twist, taper, and aeroelasticity.

Based upon a drag formulation by Eqs. (3–5), the glide polar at sea level may be written as

$$\hat{w} = (C_D/C_L)\,\hat{u} = K_3\hat{u}^{3-\gamma} + (K_4/\hat{u}) \tag{6a}$$

$$K_3 = (\hat{\rho}A_0K_1)/(2m) \tag{6b}$$

$$K_4 = (2mK_2)/(\hat{\rho}A_0) \tag{6c}$$

If we expand Eqs. (6) in a Taylor series about some optimal speed-to-fly in still air, $\hat{u} = \hat{U}$, then the glide polar is quadratic to second order according to

$$K_3\hat{u}^{3-\gamma} + (K_4/\hat{u}) \to \hat{a}\hat{u}^2 + \hat{b}\hat{u} + \hat{c} \tag{7}$$

where

$$\hat{a} = (3-\gamma)(2-\gamma)\,K_3\hat{U}^{1-\gamma} + (2K_4/\hat{U}^3)$$

$$\hat{b} = (3-\gamma)K_3\hat{U}^{2-\gamma} - (K_4/\hat{U}) - 2\hat{U}\hat{a}$$

$$\hat{c} = K_3\hat{U}^{3-\gamma} + (K_4/\hat{U}) + \hat{a}\hat{U}^2 - \hat{b}\hat{U}$$

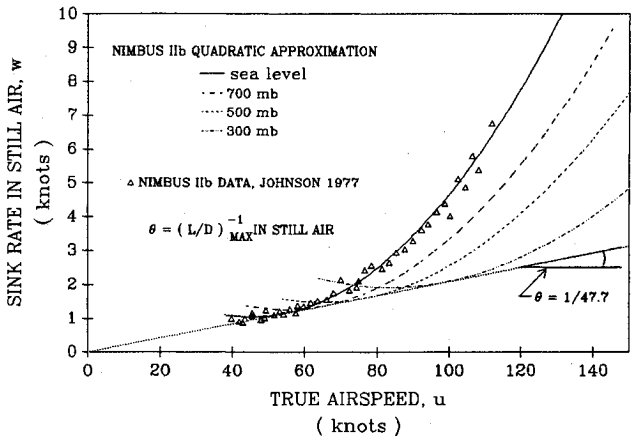

Fig. 2 Quadratic approximation to glide polar data at sea level and at altitude.

Here $\hat{a}$, $\hat{b}$, and $\hat{c}$ are based on the air density at sea level. We may then correct the quadratic glide polar in Eq. (7) to any altitude where the air density is ρ by taking

$$w = au^2 + bu + c \tag{8a}$$

$$a = \hat{a}\,(\hat{\rho}/\rho)^{-1/2} \tag{8b}$$

$$b = \hat{b} \tag{8c}$$

$$c = \hat{c}\,(\hat{\rho}/\rho)^{1/2} \tag{8d}$$

A comparison is shown in Fig. 2 between the quadratic approximation according to Eq. (7) and measured glide polar data for the test aircraft, a Schempp-Hirth Nimbus IIb, taken from Johnson[8] and corrected to sea level. The solid curve is a least-squares best fit of a quadratic to the data. The values for the sea level polar coefficients that result from this fit are

$$\hat{a} = 0.0012155\ \text{kt}^{-1} \tag{9a}$$

$$\hat{b} = -0.1106912 \tag{9b}$$

$$\hat{c} = 3.564157\ \text{kt} \tag{9c}$$

Corrected glide polars for the 700-, 500-, and 300-mb altitudes are also shown in Fig. 2 as dashed and dotted curves. Note that the maximum inverse glide slope of 47.7 remains unchanged with altitude for still air. The deformation of the polar at altitude is equivalent to increasing the wing loading by factors of 1.20, 1.42, and 1.84 for the 700-, 500-, and 300-mb levels, respectively.

With Eq. (2) expressed in terms of Eqs. (8), the inverse glide slope is reduced to dependence on four variables, u, v, α, S. Consequently, incremental changes in L/D are expressed as

$$d(L/D) = \frac{\partial(L/D)}{\partial u}\,du + \frac{\partial(L/D)}{\partial v}\,dv + \frac{\partial(L/D)}{\partial \alpha}\,d\alpha + \frac{\partial(L/D)}{\partial S}\,dS \tag{10}$$

Now, each of the variables in Eq. (10) changes with incremental changes in position along the flight path dx according to characteristic length scales. The air mass sink rates vary over distances comparable to the wave length, $\mathcal{O}(\lambda/2\pi)$, of the lee waves. The wind speed and direction vary over the lowest mode length scales of the upper level storms, typically the Rossby radius of deformation, $\mathcal{O}(R)$, as discussed in Ref. 5. On the other hand, the horizontal component of the glide velocity can vary over distances of only a few cord lengths, $\mathcal{O}(nl)$, where $n \sim 5$ according to Ref. 9. Therefore, the relative sizes of the terms in Eq. (10) are:

$$\frac{\partial(L/D)}{\partial u}\,du = \frac{\partial(L/D)}{\partial u}\frac{\partial u}{\partial x}\,dx = \mathcal{O}\left(\frac{dx}{nl}\right) \tag{11a}$$

$$\frac{\partial(L/D)}{\partial v}\,dv = \frac{\partial(L/D)}{\partial v}\frac{\partial v}{\partial x}\,dx = \mathcal{O}\left(\frac{dx}{R}\right) \tag{11b}$$

$$\frac{\partial(L/D)}{\partial \alpha}\,d\alpha = \frac{\partial(L/D)}{\partial \alpha}\frac{\partial \alpha}{\partial x}\,dx = \mathcal{O}\left(\frac{dx}{R}\right) \tag{11c}$$

$$\frac{\partial(L/D)}{\partial S}\,dS = \frac{\partial(L/D)}{\partial S}\frac{\partial S}{\partial x}\,dx = \mathcal{O}\left(\frac{2\pi\,dx}{\lambda}\right) \tag{11d}$$

In the atmosphere, $R \sim \mathcal{O}(100$ n.mi.), whereas $\lambda \sim \mathcal{O}(10$ n.mi.) for hydrostatic lee waves or $\lambda \sim \mathcal{O}(1$ n.mi.) for non-hydrostatic lee waves. These are immense compared to the wing cord. Therefore, changes in L/D with respect to wind speed, direction, and air mass sink rate are negligible compared to those with respect to changes in glide speed over any incremental distance dx. Hence, the speed-to-fly U, which maximizes the L/D over the ground, is given to $\mathcal{O}(2\pi nl/\lambda)$ accuracy by

$$\frac{\partial}{\partial u}\frac{L}{D} = 0 \text{ at } u = U \tag{12}$$

Equation (12) yields the general speed-to-fly equation for glides skewed relative to the wind, which may be written as

$$-aU^3 - 2avU\cos\alpha\sqrt{U^2 - v^2\sin^2\alpha} + (c + S + 2av^2\sin^2\alpha)\,U - vb\cos\alpha\sqrt{U^2 - v^2\sin^2\alpha} + v^2 b\sin^2\alpha = 0 \tag{13}$$

The transcendental nature of the general speed-to-fly equation [Eq. (13)] follows from the fact that speed-to-fly is a function of the crab angle by way of Eqs. (2) and (12), and crab angle is, in turn, a function of speed-to-fly as required by Eq. (1). Analytic solutions to Eq. (13) arise in the asymptotic limit of an indefinitely small crosswind component, $U^2 \gg v^2\sin^2\alpha$, for which the speed-to-fly $u = U_0$ is given by

$$U_0^3 + p_0 U_0^2 + q_0 U_0 + r_0 = 0 \tag{14}$$

where

$$p_0 = 2v_0\cos\alpha$$

$$q_0 = [-(c + S + 2av_0^2\sin^2\alpha - v_0 b\cos\alpha)/a]$$

$$r_0 = (v_0^2 b\sin^2\alpha/a)$$

$$v_0 = v \ll \sqrt{U_0^2/\sin^2\alpha}$$

The speed-to-fly equation thus collapses to an ordinary cubic equation for weak crosswinds, yielding the following solution:

$$U_0 = \left[-\frac{d_0}{2} + \sqrt{\frac{d_0^2}{4} + \frac{f_0^3}{27}}\right]^{1/3} + \left[-\frac{d_0}{2} - \sqrt{\frac{d_0^2}{4} + \frac{f_0^3}{27}}\right]^{1/3} - \frac{2v_0\cos\alpha}{3} \tag{15}$$

where

$$d_0 = (1/27)(2p_0^3 - 9p_0 q_0 + 27r_0)$$

$$f_0 = (1/3)(3q_0 - p_0^2)$$

The remaining two roots of Eq. (14) are less than zero (backwards flight) and are therefore not sensible. As a particular case of Eq. (15), the speed-to-fly solution in a direct headwind or tailwind ($\alpha = 0$), which corresponds to the graphical result by tangent plotting due to Kuettner,[3] is found to be

$$U_0(\alpha = 0) = (1/2a)[4a^2v^2 + 4a(c + S - bv)]^{1/2} - v \qquad (16)$$

For a general solution to Eq. (13), a seeded iteration is begun from the weak crosswind solution U_0 for some small wind speed $v = v_0$. With each iterative step n thereafter, the wind speed is stepped incrementally by $n\delta v$. The numerical computations for any given step n are based on a Taylor series expansion of $(U^2 - v^2 \sin^2\alpha)^{1/2}$ about the speed-to-fly solution from the previous iteration, $U = U_{n-1}$. By this numerical scheme, the general speed-to-fly equation for the nth iteration is

$$U_n^3 + p_n U_n^2 + q_n U_n + r_n = 0 \qquad (17a)$$

where

$$p_n = \frac{\{-vb\cos\alpha[(1/2)\eta^{-1/2} - (1/2)U_{n-1}^2\eta^{-3/2}] - 2av\cos\alpha(U_{n-1}^3\eta^{-3/2})\}}{\{-a - av\cos\alpha(\eta^{-1/2} - U_{n-1}^2\eta^{-3/2})\}} \qquad (17b)$$

$$q_n = \frac{\{c + S + 2av^2\sin^2\alpha - vb\cos\alpha U_{n-1}^3\eta^{-3/2} - 2av\cos\alpha[\eta^{1/2} - (1/2)U_{n-1}^2\eta^{-1/2} - (1/2)U_{n-1}^4\eta^{-3/2}]\}}{\{-a - av\cos\alpha(\eta^{-1/2} - U_{n-1}^2\eta^{-3/2})\}} \qquad (17c)$$

$$r_n = \frac{\{v^2b\sin^2\alpha - vb\cos\alpha[\eta^{1/2} - (1/2)U_{n-1}^2\eta^{-1/2} - (1/2)U_{n-1}^4\eta^{-3/2}]\}}{\{-a - av\cos\alpha(\eta^{-1/2} - U_{n-1}^2\eta^{-3/2})\}} \qquad (17d)$$

where $n = 1,2,3\ldots$; $\eta = U_{n-1}^2 - v^2\sin^2\alpha$; $v = v_0 + n\delta v$. Hence, the general speed-to-fly solution for any given wind speed and arbitrary α is given by

$$U_n = \left[-\frac{d_n}{2} + \sqrt{\frac{d_n^2}{4} + \frac{f_n^3}{27}}\right]^{1/3} + \left[-\frac{d_n}{2} - \sqrt{\frac{d_n^2}{4} + \frac{f_n^3}{27}}\right]^{1/3} - \frac{2v\cos\alpha}{3} \qquad (18)$$

where $d_n = (1/27)(2p_n^3 - 9p_nq_n + 27r_n)$; $f_n = (1/3)(3q_n - p_n^2)$; $n = 1,2,3,\ldots$. Again, the two remaining roots to Eq. (17a) are less than zero and consequently have no physical significance.

Numerical Results

The general speed-to-fly solutions for arbitrary wind speed and direction were computed between the 700- and 300-mb levels by seeded iterations using Eqs. (14–18). The computations were based on an unballasted Nimbus IIb glide polar according to Eqs. (8) and (9). The computational sweeps were stepped in both the positive and negative wind directions using increments of $\delta v = 1.0$ kt. This procedure was selected in preference to some general iterative search routine because the speed-to-fly equation [Eq. (13)] has multiple roots and it was desirable to find cause and effect relationships between speed-to-fly, optimal crab angle, air mass movements, and altitude effects on the glide polar.

The speed-to-fly and optimal crab angle dependence on the wind speed and direction is computed in Fig. 3 for the 700-mb level and in Fig. 4 for the 300-mb level. These computations assume no net vertical motion in the atmosphere, $S = 0$, as would generally be the case during long glides in between wave generating mountains. Negative wind speeds correspond to headwinds, whereas positive values denote tailwinds. Positive crab angles denote deviations from the course line in the same sense as the wind vector (headwinds), whereas negative crab angles deviate from the course line against the wind angle (tailwinds). The fastest and slowest speeds-to-fly arise from glides directly against and with the wind ($\alpha = 0$), respectively. The speed-to-fly in a direct crosswind ($\alpha = 90$ deg) is a symmetric function about zero wind speed and is slower than all headwind cases and faster than all tailwind cases. All remaining possible crosswind solutions are intermediate between these two extremes, with small differences among skewed glides into the wind, but significantly faster speeds-to-fly for increasing crosswind components with the wind. When $0 < \alpha < 90$ deg, the maximum inverse glide slopes apparently result from keeping the crab angle small, $\beta < \Theta(45$ deg). Hence, the speeds-to-fly during skewed glides with the wind increase with increasing crosswind component in order to maintain the course line without resorting to exceedingly large crab angles.

It is also interesting to note from Figs. 3 and 4 that the indicated speed to fly (based on pitot-static airspeed systems) varies with altitude for any given wind speed and direction. This effect was not considered by MacCready.[1,2] Generally, slower indicated airspeeds are required at higher altitudes for any nonzero wind speed regardless of direction. Consequently, the indicated speeds-to-fly and crab angles for 60-kt winds at 700-mb are comparable to those required for 90-kt winds at the 300-mb level. The true speeds-to-fly increase with increasing altitudes but by less than a constant factor $(\hat{\rho}/\rho)^{1/2}$. This results from the fact that the higher effective wing loading at altitude enables more efficient penetration into a headwind component but requires slower glides at a higher C_L with a tailwind component in order to minimize an already high relative sinking speed.

In Fig. 5, a comparison is made of the maximum possible inverse glide slopes between the 700- and 300-mb levels if exact

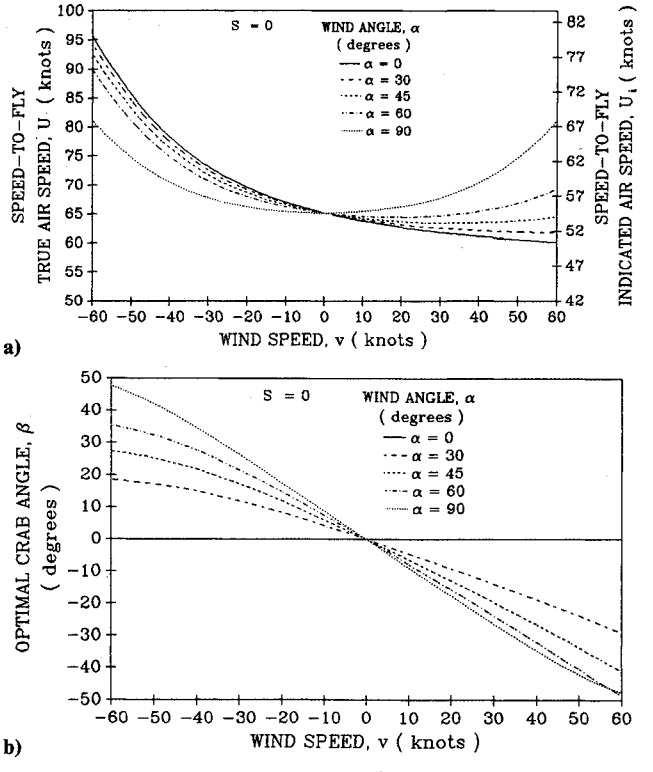

Fig. 3 Speed-to-fly and crab angle vs winds at 700 mb.

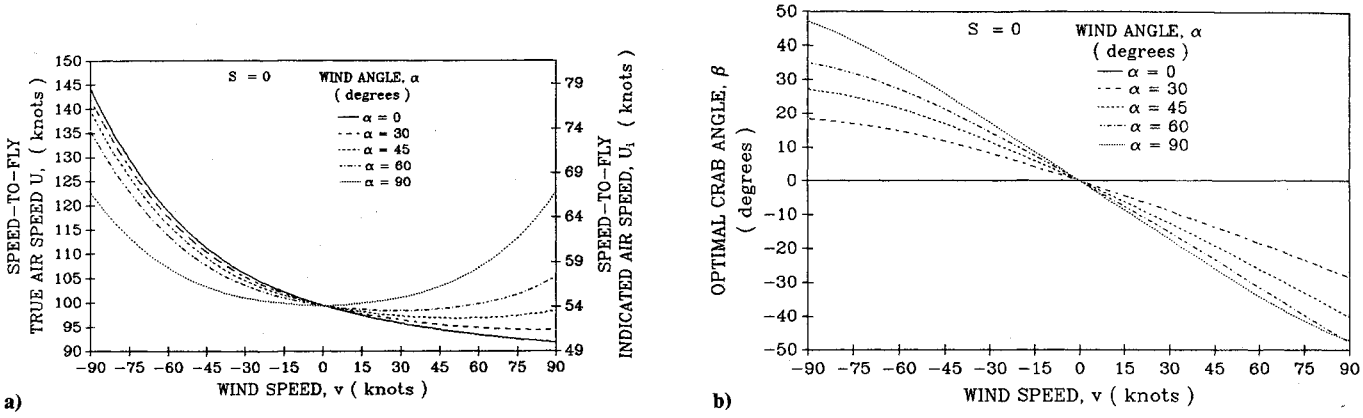

Fig. 4 Speed-to-fly and crab angle vs winds at 300 mb.

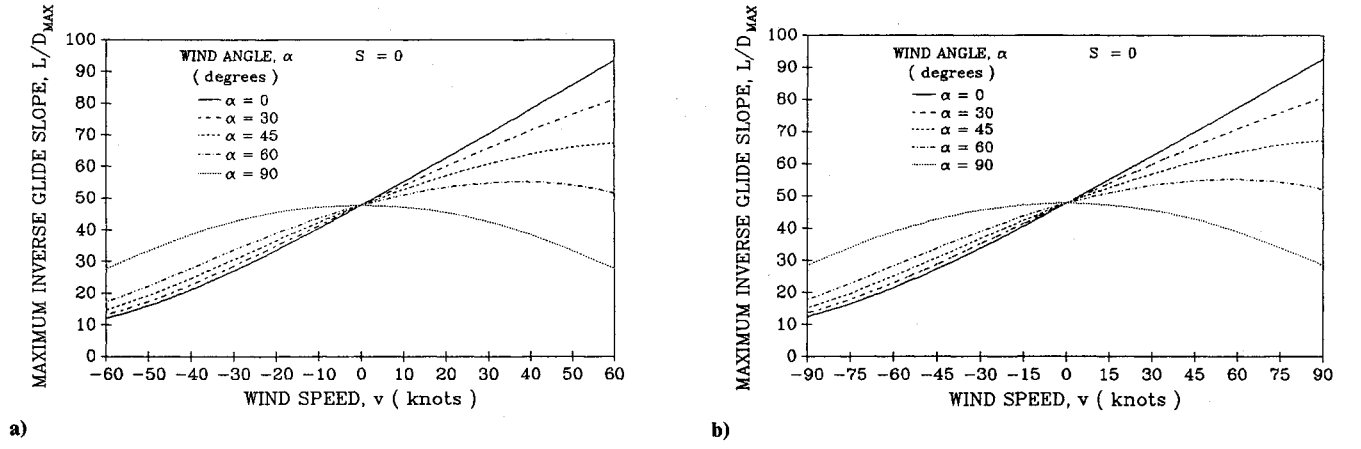

Fig. 5 Maximum inverse glide slopes vs winds at 700 and 300 mb.

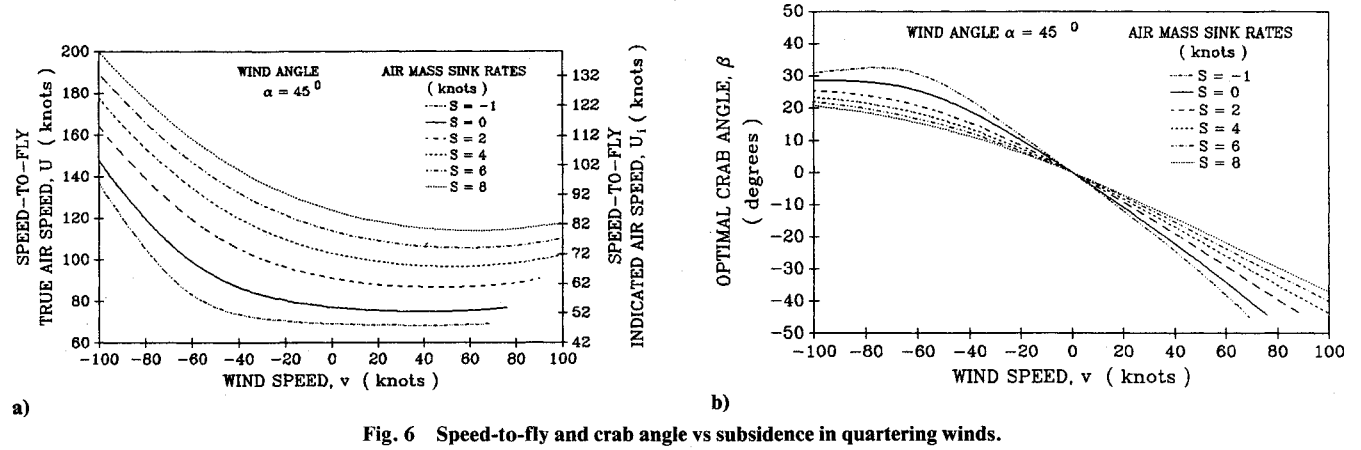

Fig. 6 Speed-to-fly and crab angle vs subsidence in quartering winds.

adherence to speed-to-fly and optimal crab angle is made according to Figs. 3 and 4. A higher L/D is possible into the wind at higher altitudes for any given headwind and direction. Nonetheless, strong headwind conditions clearly should be avoided, as the L/D falls catastrophically from 47.7 in still air to less than 15. Conversely, flatter glide slopes are achieved for any given tailwind and direction at lower altitudes. In a direct crosswind, $\alpha = 90$ deg, it is clearly advantageous to fly at a higher altitude for any given wind speed. Again, the inverse glide slopes for 60-kt winds at 700-mb are found to be comparable to those in 90 kt of wind at the 300-mb level. These features are consistent with the fact that a higher effective wing loading at higher altitudes is an advantage when penetrating into the wind or in strong crosswinds but a disadvantage when gliding slowly at minimum relative sinking speeds with the wind. Even so, a 90-kt direct tailwind at 300 mb will improve the L/D from 47.7 in still air to 92.7. This value degrades to 65.0 if the 300-mb winds become quartering tailwinds, $\alpha = 45$ deg.

Figure 6 shows computations of speed-to-fly and optimal crab angles for the case of quartering headwinds and tailwinds at the 500-mb level when vertical air mass movements are encountered. Contour plots are shown for particular air mass sink rates of $-1.0 \leq S \leq 8.0$ kt, as would be typically encountered while traversing mountains in fields of lee waves. Computations for an air mass rising faster than the aircraft's minimum relative sinking speed are not possible because a state of perpetual motion is achieved at the start of the seeded iteration, $v = v_0$, for which the problem has not been correctly posed by Eq. (12). The problem in this case becomes one of

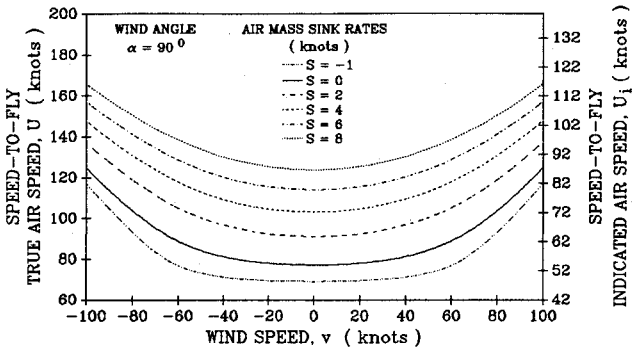

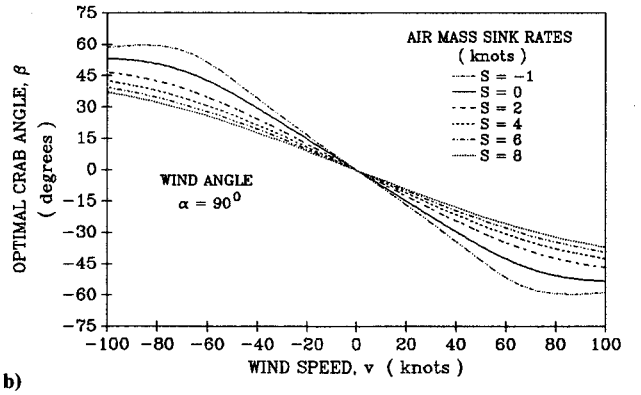

Fig. 7 Speed-to-fly and crab angle vs subsidence in direct crosswinds.

maximizing climb rate for which the speed to fly is $U \rightarrow u_s$. Otherwise, the speed-to-fly solutions in Fig. 6 require one to speed up in sinking air and to slow down in rising air, similar to MacCready.[1,2] However, unlike MacCready's original result, the speeds-to-fly for any given air mass sink rate are dependent upon the wind speed, requiring faster glides for a headwind component and slower glides with a tailwind component. Regardless of the air mass sink rate, speeds-to-fly in strong quartering tailwinds tend to increase slightly with increasing wind speed in order to prevent glide slope degradation resulting from large crab angles, $\beta > \mathcal{O}(45 \text{ deg})$. This result is a modification to Kuettner's original downwind strategy (see Ref. 3). In strong quartering headwinds with a rapidly sinking air mass, one finds in Figs. 6 that rather large speeds to fly, $\mathcal{O}(200 \text{ kt})$, are required that exceed the structural load limits of the test aircraft. In 1-kt rising air with a quartering tailwind, the speed-to-fly is less than the best L/D speed for still air.

Figure 7 shows the effect of vertical air mass movements on speeds-to-fly and optimal crab angles in direct crosswinds at the 500-mb level. In strong wind with rapidly sinking air, the speeds-to-fly are significantly less than the corresponding quartering headwind cases in Fig. 6 but also significantly greater than the corresponding tailwind cases. For weak direct crosswinds ($v < 30$ kt) there is little change in speed to fly with increasing or decreasing wind speed since most of the compensation is done with the crab angle. Unlike all other cases considered, the optimal crab angle for strong direct crosswinds ($v > 60$ kt) does indeed exceed 45 deg in nonsinking air.

Figure 8 shows the maximum obtainable inverse glide slopes with vertical air mass motion in quartering headwinds and tailwinds and in direct crosswinds at the 500-mb level. The computations are based on exact adherence to speed to fly and optimal crab angle according to Figs. 6 and 7. One finds that slowly rising air, $S = -1.0$ kt, yields impressive L/D for both strong quartering tailwinds ($L/D \approx 190$) as well as weak crosswinds ($L/D \approx 140$). However, strong quartering headwinds degrade the L/D to < 10 regardless of the vertical air mass motions. In fact, the inverse glide slope in this case is almost as bad for 8 kt of air mass sink as it would be for nonsinking air. The degradation in L/D for strong direct crosswinds is only slightly less. For weak quartering headwinds/tailwinds and direct crosswinds, any rate of sinking of the air mass exerts a pronounced reduction in L/D compared to the case $S = 0$. Most of this performance loss occurs during the first few knots of air mass sink. Very little additional loss occurs for $S \geq 4.0$ kt.

Experiment

To ascertain the accuracy of the speed-to-fly and optimal crab angle computations, a series of test flights were conducted with an unballasted Nimbus IIb. The test flights were performed using the active lee wave generating topography of the Laguna Mountains in Southern California. Wave entry was accomplished by aerotow to a point in the neighborhood of the Julian VORTAC. Upon release, climb was initiated to the 500-mb level according to visual flight rules, with additional climbs to the 300-mb level upon receipt of clearance from the Los Angeles Center. After reaching maximum permissible altitude, the test aircraft departed the wave generating region for a series of way points whose exact position was known. The altitude lost in gliding between the way points was recorded by means of a precision barograph and used together with the known distances between way points to calculate the inverse glide slope with respect to the ground. Passage over each way point was determined by visual recognition and annotated on the barograph by executing a rapid dive and recovery maneuver to produce a mark on the trace known as a "notch."

Wind data for the tests were derived from National Weather Service soundings at San Diego, California, and Blythe, Arizona. Test flights were conducted about the 700- , 500- , and 300-mb levels for which sounding data and forecast charts were available. Way points were selected with separations

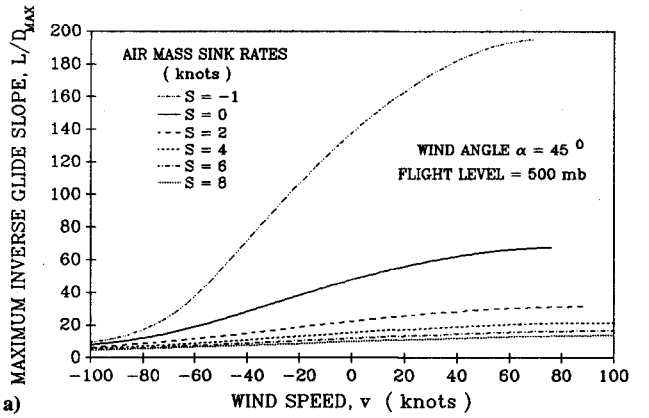

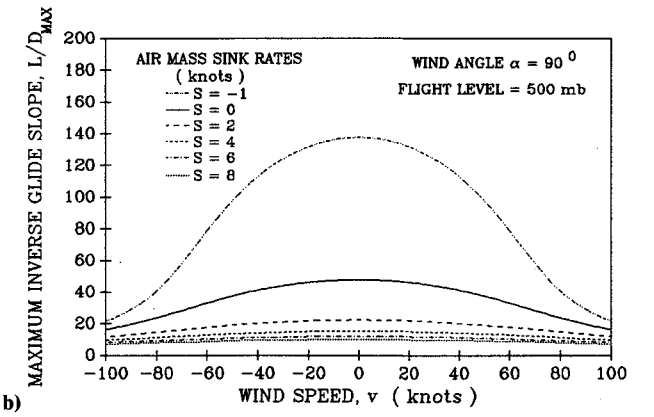

Fig. 8 Maximum inverse glide slopes vs subsidence in quartering and direct crosswinds.

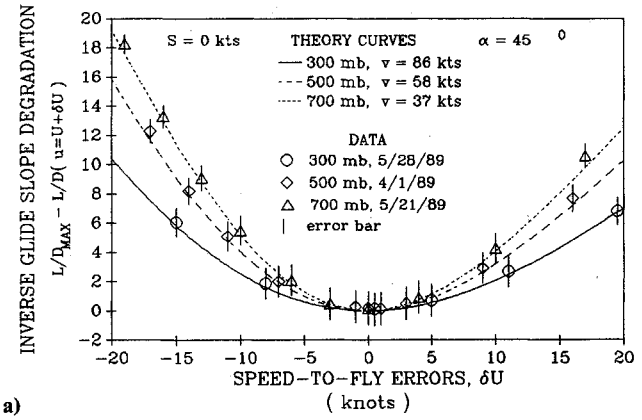

a)

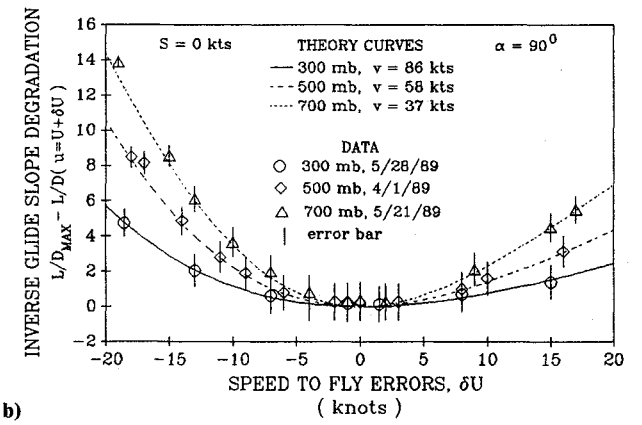

b)

Fig. 9 Effects of speed-to-fly errors in quartering tailwinds and direct crosswinds.

ranging from 11.4 to 37.8 statute miles so that the maximum altitude variance about any one of these levels did not exceed ± 2000 ft. Since the test aircraft lacked accurate positioning equipment, no attempt was made to test speed-to-fly theories within the variable vertical velocities of the lee wave field. Instead, the way points were selected upwind of the wave generating topography to test the direct crosswind calculations and a considerable distance downwind of the wave generating topography for quartering tailwind tests. This arrangement was aided by the fact that the lee waves were generated over a broad tilted plateau and were, therefore, essentially hydrostatic in nature with vertically upward propagation and no secondary or tertiary phases downwind (see Ref. 5).

Figure 9 shows the results of these tests during which known speed-to-fly errors δU were flown to yield measured inverse glide slopes $L/D(u = U + \delta U)$. The speed-to-fly errors are corrected for the airspeed system errors measured by Johnson.[8] In every case for which a nonzero speed-to-fly error was flown, the resulting inverse glide slopes are found to be less than the theoretical maximum L/D_{max} when exact adherence to speed-to-fly and optimal crab angle is maintained. The curves in Fig. 9 are generated by a numerical search about either side of the speed-to-fly solutions computed from Eqs. (14–18) for the respective altitudes and winds. The particular wind speeds for those computations are selected in between the San Diego and Blythe soundings based on a minimization of the variance between the data and resulting theory curves. A check of the L/D_{max} values is provided by the data points gathered for zero speed-to-fly errors. The loss in L/D due to any given speed-to-fly error is greater at lower altitudes for both quartering tailwinds and direct crosswinds. Furthermore, flying too slowly produces a greater degradation in L/D than flying too fast. Speed-to-fly errors have a greater adverse impact in quartering tailwinds than in direct crosswinds. However, in either case, the speed-to-fly errors resulting from flying too slowly can diminish the L/D by 15 points or more. This is equivalent to turning the clock on aerodynamic design back by as much as 50 years. In other words, pilotage must be considered a leading-order process.

Conclusions

1) Speed-to-fly during glides skewed relative to the wind by less than 90 deg requires flying faster through sinking air or into a headwind component and flying slower through rising air or with a tailwind component such that the crab angle does not become excessively large, $\beta < \Theta(45 \text{ deg})$.

2) Speed-to-fly in direct crosswinds requires flying faster through sinking air or with increasing wind speed and flying slower through rising air or with decreasing wind speed, using crab angles that may exceed 45 deg for the case of strong winds in a nonsinking air mass.

3) Maximum L/D with any given tailwind component is achieved at lower altitudes.

4) Maximum L/D with any given headwind component or any given direct crosswind is achieved at higher altitudes.

5) Speed-to-fly errors resulting from flying too slowly yield the greatest losses in L/D.

6) Losses in L/D for any given speed-to-fly error are greater at lower altitudes.

Acknowledgments

This work was partially supported by a grant from the Office of Naval Research, Code 1121. The authors are grateful for the thoughtful criticisms provided by the reviewers, which led to the formulation of Fig. 1.

References

[1]MacCready, P. B., "Optimum Airspeed Selector," *Soaring,* Vol. 18, No. 2, 1954, pp. 16–21.

[2]MacCready, P. B., "Understanding Speed-to-Fly and the Speed Ring," *Soaring,* Vol. 47, No. 5, 1982, pp. 42–47.

[3]Kuettner, J. P., "The 2000 Kilometer Wave Flight-Part II," *Soaring,* Vol. 49, No. 3, 1985, pp. 22–27.

[4]Reichmann, H., *Cross-Country Soaring,* Thomson, Pacific Palisades, CA, 1978, p. 98.

[5]Gill, A. E., *Atmosphere—Ocean Dynamics,* Academic, Orlando, FL, 1982, pp. 274–294.

[6]Prandtl, L., *Abriss der Stromungslegre,* Vieweg, Braunschweig, FRG, 1931, p. 189.

[7]Van Dyke, M., "Lifting Line Theory as a Singular-Perturbation Problem," *Journal of Applied Mathematics and Mechanics,* Vol. 28, 1964, pp. 90–101.

[8]Johnson, R. H., "Flight Test Polar Measurements of Modern Sailplanes," *Technical Soaring,* Vol. 4, No. 4, 1977, pp. 13–27.

[9]Basu, B. C., and Hancock, G. J., "The Unsteady Motion of a Two-Dimensional Aerofoil in Incompressible Inviscid Flow," *Journal of Fluid Mechanics,* Vol. 87, No. 1, 1978, pp. 159–178.